Differential antitumor activity of compounds targeting the ubiquitin-proteasome machinery in gastrointestinal stromal tumors (GIST)

Jessica L. Rausch,[1] Areej A. Ali,[1] Donna M. Lee,[1] Yemarshet K. Gebreyohannes,[2] Keith R. Mehalek,[1] Aya Agha,[1] Sneha S. Patil,[1] Yanis Tolstov,[3] Jasmien Wellens,[2] Harbir S. Dhillon,[1] Kathleen R. Makielski,[1] Maria Debiec-Rychter,[4] Patrick Schöffski,[2] Agnieszka Wozniak,[2] Anette Duensing[1,5,*]

[1]Cancer Therapeutics Program
UPMC Hillman Cancer Center
Pittsburgh, PA, USA

[2]Departments of Oncology and General Medical Oncology
University Hospitals Leuven and KU Leuven, Leuven Cancer Institute
Leuven, Belgium

[3]Molecular Urooncology
University of Heidelberg School of Medicine
Heidelberg, Germany

[4]Department of Human Genetics
University Hospitals Leuven and KU Leuven
Leuven, Belgium

[5]Department of Pathology
University of Pittsburgh School of Medicine
Pittsburgh, PA, USA

Corresponding author:
Anette Duensing, MD; UPMC Hillman Cancer Center; Research Pavilion, Suite G.17; 5117 Centre Avenue; Pittsburgh, PA 15213; USA.
Phone: +1-412-623-5870; Fax: +1-412-623-1010; E-mail: aduensin@pitt.edu

ABSTRACT

The majority of gastrointestinal stromal tumors (GISTs) are driven by oncogenic KIT signaling and can therefore be effectively treated with the tyrosine kinase inhibitor (TKI) imatinib mesylate. However, most GISTs develop imatinib resistance through secondary *KIT* mutations. The type of resistance mutation determines sensitivity to approved second-/third-line TKIs but can show high inter- and intratumoral heterogeneity. Therefore, therapeutic strategies that target KIT independently of the mutational status are intriguing. Inhibiting the ubiquitin-proteasome machinery with bortezomib is effective in GIST cells through a dual mechanism of *KIT* transcriptional downregulation and upregulation of the pro-apoptotic histone H2AX but clinically problematic due to the drug's adverse effects. We therefore tested second-generation inhibitors of the 20S proteasome (delanzomib, carfilzomib and ixazomib) with better pharmacologic profiles as well as compounds targeting regulators of ubiquitination (b-AP15, MLN4924) for their effectiveness and mechanism of action in GIST. All three 20S proteasome inhibitors were highly effective *in vitro* and *in vivo*, including in imatinib-resistant models. In contrast, b-AP15 and MLN4924 were only effective at high concentrations or had mostly cytostatic effects, respectively. Our results confirm 20S proteasome inhibitors as promising strategy to overcome TKI resistance in GIST, while highlighting the complexity of the ubiquitin-proteasome machinery as therapeutic target.

INTRODUCTION

The majority of gastrointestinal stromal tumors (GISTs) are driven by an oncogenic mutation that constitutively activates the KIT or PDGFRA (platelet-derived growth factor receptor alpha) receptor tyrosine kinase. This leads to ligand-independent activation of the receptor as well as downstream signaling cascades that promote tumor cell proliferation and survival. The tyrosine kinase inhibitor (TKI) imatinib mesylate (Gleevec®) is a highly effective first-line drug for the treatment of inoperable or metastatic GIST. Nevertheless, there is a need for new therapeutic approaches, because resistance to imatinib develops in approximately 50% of patients within the first two years of treatment [1]. In this scenario, the FDA-approved second- and third-line drugs sunitinib and regorafenib offer little additional benefit [2].

The major mechanism of TKI resistance in GIST involves secondary mutations in the kinase domain of the primarily affected kinase indicating the continued dependency on KIT/PDGFRA kinase activation. Therefore, therapeutic strategies targeting these kinases without the need of kinase domain binding seem particularly promising.

The 26S proteasome is a 2.5 MDa multiprotein complex and the main protein degradation machinery of eukaryotic cells [3]. It consists of a 20S tube-like proteolytic core particle and two 19S regulatory particles at either end. Proteins destined to be degraded are selectively targeted to the proteasome by the addition of a series of covalently attached ubiquitin molecules. Deubiquitinating enzymes associated with the 19S regulatory subunit remove these ubiquitin chains before proteins can enter the proteolytic subunit. The 20S core contains three major proteolytic activities (β5 chymotrypsin-like, β1 caspase-like and β2 trypsin-like), which together yield peptides that are three to 25 amino acids in length. Inhibitors of the 20S proteasome core particle, such as the prototype proteasome inhibitor bortezomib (Velcade®), have gained clinical importance for the

treatment of multiple myeloma and certain lymphomas [4].

Previous studies from our laboratory have shown that targeting the ubiquitin-proteasome machinery with bortezomib is highly effective in GIST cells. Importantly, this was independent of *KIT* mutational status [5]. We could demonstrate that bortezomib-induced apoptosis is mediated by a dual mechanism of action. Inhibition of the proteolytic machinery leads to increased levels of soluble, non-chromatin-bound pro-apoptotic histone H2AX [5–7]. In addition, a dramatic downregulation of KIT expression is mediated by inhibition of active gene transcription [5]. It is known that loss of KIT expression, e.g. *via* siRNA-mediated knockdown or HSP90 inhibition, is a strong inducer of apoptosis in GIST cells [6,8]. Although bortezomib has not shown significant clinical activity in many solid tumors, including an array of sarcomas [9], there are a number of recent reports of bortezomib's clinical activity in GIST. For example, a GIST patient had the most significant response, an approximately 36% tumor shrinkage (WHO criteria), in a study evaluating bortezomib as a daily subcutaneous regimen in various solid tumors [10]. In another study testing bortezomib in combination with vorinostat, one of the two GIST patients included in the cohort achieved stable disease (SD) [11]. Nevertheless, bortezomib is associated with marked adverse effects, warranting the evaluation of second-generation proteasome inhibitors [10,12].

Carfilzomib (Kyprolis®, PR-171), ixazomib (Ninlaro®, MLN-9708), and delanzomib (CEP-18770) are inhibitors of the 20S proteolytic core particle of the 26S proteasome, like bortezomib [4]. Carfilzomib is an intravenously administered tetrapeptide epoxyketone that differs structurally and mechanistically from bortezomib [13]. Approved by the FDA in 2012 for therapy-resistant multiple myeloma [14], it inhibits the β5 chymotrypsin-like subunit of the proteasome, similar to bortezomib, but does so irreversibly and with a higher selectivity [13]. Together with the notion that carfilzomib has less off-target effects, these facts may explain its efficacy in bortezomib-resistant cells as well as a lesser degree of adverse

effects [13,15]. Ixazomib is the first orally bioavailable inhibitor of the 20S proteasome [16]. It is a structural derivative of bortezomib with improved pharmacologic properties and reversibly inhibits the chymotrypsin-like β5 subunit of the 20S proteasome [14–16]. Ixazomib was recently approved for the treatment of multiple myeloma [17]. Delanzomib is a reversible P2 threonine boronic acid proteasome inhibitor that can be administered orally and intravenously [18,19]. It potently inhibits the β5 chymotrypsin-like and the β1 caspase-like subunit of the proteasome. Compared to bortezomib, delanzomib exhibits a more sustained inhibition of proteasome activity in multiple myeloma cells [18,19]. Results of a phase I/II clinical trial in relapsed and refractory multiple myeloma were recently reported [20,21].

In addition to inhibitors of the proteolytic 20S core of the proteasome, several regulators of the proteasomal degradation process have recently emerged as therapeutic targets. Deubiquitinase enzymes (DUBs) catalyze the cleavage of ubiquitin from proteasome-targeted, ubiquitin-conjugated proteins at the 19S regulatory core particle of the 26S proteasome [3]. b-AP15 is a DUB inhibitor that interferes with the activity of the ubiquitin-specific peptidase 14 (USP14) and ubiquitin carboxyl-terminal hydrolase isozyme L5 (UCHL5) [21,22]. As a result, b-AP15 leads to rapid accumulation of high molecular weight ubiquitin conjugates, triggering a functional shutdown of the proteasome [22]. Importantly, b-AP15 has shown pre-clinical activity in multiple myeloma and Waldenström's macroglobulinaemia [23,24].

A second important regulatory process of the proteolytic machinery involves the small ubiquitin-like modifier NEDD8 [25]. NEDD8 is attached to lysine residues of proteins in a similar fashion as ubiquitin, and "neddylation" has been specifically implicated in regulating the turnover of cell cycle-regulatory proteins, such as $p27^{Kip1}$ [26,27]. Neddylation of the cullin subunits of cullin-based E3 ubiquitin ligases is critical for the recruitment of the E2 ubiquitin-conjugating enzyme facilitating ubiquitin conjugation [26,27]. Inhibition of

neddylation hence leads to reduced protein degradation *via* reduced ubiquitination and targeting to the proteasome, while proteasome activity itself stays intact. MLN4924 (Pevonedistat®) is the first-in-class inhibitor of this process, targeting the NEDD8 activating enzyme (NAE) [28]. It has shown pre-clinical activity in various solid tumors and hematologic malignancies and is currently in several clinical trials, including a Phase 3 study in hematological malignancies (NCT03268954).

In the present study, we could show that all three inhibitors of the 20S proteolytic core of the proteasome were highly effective in GIST cells. Their effectiveness was not affected by *KIT* mutational status or sensitivity to imatinib. Mechanistically, the pro-apoptotic activity of these compounds was mediated by a dual mechanism identical to bortezomib that resulted in upregulation of histone H2AX and transcriptional inhibition of *KIT*. Of note, delanzomib was the most effective compound tested. By contrast, the DUB inhibitor b-AP15 and the NEDD8 activating enzyme inhibitor MLN4924 had a substantially lesser effect on cell proliferation and induction of apoptosis. In summary, targeting the proteolytic 20S core unit of the proteasome in GIST could be a promising therapeutic strategy in TKI-resistant GISTs.

RESULTS

The second-generation inhibitors of the 20S proteasome carfilzomib, ixazomib and delanzomib effectively induce apoptosis and cell cycle arrest in GIST cells

To determine whether carfilzomib, ixazomib and delanzomib have an effect on GIST cell viability and/or apoptosis, IM-sensitive (GIST882, GIST-T1) and IM-resistant (GIST48, GIST430) GIST cell lines were treated with increasing concentrations covering a 100,000-fold concentration range (0.1 nM – 10.0 µM). Cell viability and caspase 3/7

activity were measured using luminescence-based assays (Fig. 1A, B; Suppl. Methods). All three compounds were highly effective with IC_{50}s as low as 9 nM (Table 1A). Of note, delanzomib was the most potent compound (IC_{50}s of 9-36 nM), whereas carfilzomib and ixazomib were approximately one order of magnitude less effective (IC_{50}s of 67-1679 nM and 41-175 nM, respectively; Table 1A). Importantly, drug response was independent of *KIT* mutational status and sensitivity to imatinib. In fact, IM-resistant cells had an overall lower IC_{50} for all drugs than IM-sensitive cells.

To biochemically assess tumor cell responses to delanzomib, carfilzomib and ixazomib, we evaluated markers of apoptosis and cell cycle regulation by immunoblot analysis (Fig. 1C, D; Suppl. Fig. 1A; Suppl. Fig. 2A; Suppl. Methods). Delanzomib had a strong pro-apoptotic activity and effectively induced cell cycle arrest at concentrations as low as 0.1 nM in IM-sensitive (GIST882, GIST-T1) and IM-resistant (GIST48, GIST430) cell lines (Fig. 1C, D; Suppl. Fig. 1A). In comparison, carfilzomib and ixazomib had a less pronounced effect on apoptosis induction and cell cycle exit (Fig. 1 D, Suppl. Fig. 2A), matching the results obtained in the luminescence-based assays (Fig. 1A, B). All assays were performed in all cell lines for the remainder of the manuscript. For clarity and briefness, representative results of one IM-sensitive and one IM-resistant cell line are shown, while all other data are included in the Supplement section.

The ability of delanzomib, carfilzomib and ixazomib to induce apoptosis was also evaluated using the TUNEL assay and confirmed the immunoblotting studies (Fig. 1E, Suppl. Fig. 1B, Suppl. Fig. 2B, C; Suppl. Methods). As expected from the previous results, carfilzomib and ixazomib were less effective (Suppl. Fig. 2B, C). Importantly however, there was generally no difference in activity between IM-sensitive and IM-resistant cells.

The effect of delanzomib, carfilzomib and ixazomib was time-dependent (Fig. 1F, Suppl. Fig. 1C, Suppl. Fig. 2D, E). Apoptosis started to be evident as early as 8 h after treatment in GIST-T1 cells (Fig. 1F, Suppl. Fig. 2D, E). Interestingly, exit from the cell

division cycle after delanzomib treatment lagged considerably. As seen before, there was no substantial difference between IM-sensitive and IM-resistant cells.

Taken together, the second-generation inhibitors of the 20S proteasome delanzomib, carfilzomib and ixazomib showed significant cytotoxic activity in GIST cells, which was independent of the *KIT* mutational status and hence imatinib sensitivity. Delanzomib was the most effective of the three compounds tested.

The ability to inhibit the activity of the proteasome and induce accumulation of ubiquitinated proteins correlates with GIST cell cytotoxicity

Delanzomib, carfilzomib and ixazomib predominantly inhibit the chymotrypsin-like activity of the 20S proteasome in multiple myeloma cells [13,14,16,18,19,29,30]. To correlate 20S proteasome inhibitory activity with their cytotoxicity in GIST cells, we measured the chymotrypsin-like activity of the 20S proteasome in a luminescence-based assay using Suc-LLVY-(succinyl-leucine-leucine-valine-tyrosine-)aminoluciferin as a substrate. While all three proteasome inhibitors strongly inhibited the proteasome, delanzomib was most effective, correlating with the compounds' ability to induce apoptosis (EC_{50}s of 5-13 nM, Table 1B). As before, no significant difference between IM-sensitive and IM-resistant GIST cells was seen. Interestingly, carfilzomib and ixazomib showed stronger proteasome inhibition capacity than delanzomib in the lower concentration range when treating IM-sensitive GIST882 and GIST-T1 cells (Fig. 2A). Together, our results indicate that the potency of proteasome inhibition indeed correlates with cytotoxic efficacy in GIST cells (Fig. 1; Suppl. Fig. 1).

In a next step, we assessed whether the accumulation of ubiquitinated proteins coincides with cytotoxicity of the compound. Indeed, treatment with delanzomib not only led to a dose-dependent accumulation of ubiquitinated proteins when measured by immunoblotting, but also had the strongest effect when compared to carfilzomib and

ixazomib (Fig. 2B; Suppl. Fig. 1D, Suppl. Fig. 3A, C). This process was remarkably fast, starting after only one hour of treatment in most cell lines (Fig. 2 C; Suppl. Fig. 1E; Suppl. Fig. 3), and was again independent of GIST mutational status and IM sensitivity. Kinase inhibitor (imatinib, sunitinib) treatments that were used as controls did not lead to increased ubiquitination, as expected.

Taken together, delanzomib, carfilzomib and ixazomib effectively inhibit the chymotrypsin-like activity of the 20S proteasome in IM-sensitive and IM-resistant GIST cells and lead to the accumulation of ubiquitinated proteins. Importantly, delanzomib had the strongest effect of the three, thereby suggesting that the cytotoxic effect of the compounds could be associated with their ability to inhibit the proteasome and induce the accumulation of ubiquitinated proteins.

Inhibition of the USP14/UCHL5 deubiquitinating enzymes or the NEDD8 activating enzyme (NAE) have a lower pro-apoptotic activity in GIST cells when compared to 20S inhibitors

Having shown that delanzomib, carfilzomib and ixazomib have activity against GIST cells, we tested whether the cytotoxic effect is 20S proteasome inhibitor-specific or whether inhibition of protein degradation by targeting regulators of the ubiquitin-proteasome pathway has the same effect.

b-AP15 is a deubiquitinase enzyme (DUB) inhibitor that has shown pre-clinical activity [23,24]. It interferes with ubiquitin cleavage from proteasome-targeted proteins at the 19S regulatory particle of the 26S proteasome, thereby leading to a functional shutdown of the proteasome [3,20]. Treatment of GIST cells with increasing concentrations of b-AP15 only resulted in a significant reduction in cell viability or increase of apoptosis at very high concentrations (1 μM and higher) as determined by luminescence-based assays (Fig. 3A, B, Suppl. Fig. 4A). IC_{50}s ranged from 0.5 μM and 1.2 μM in IM-resistant cells (GIST48

and GIST430, respectively) to over $8x10^{18}$ μM in IM-sensitive cells (GIST882; Table 1C). As expected, immunoblot analysis paralleled these results (Fig. 3B). While b-AP15 did lead to the accumulation of ubiquitinated proteins, concentrations of 1.0 μM or higher were needed to achieve this effect (Fig. 3C).

We then tested the NEDD8 activating enzyme (NAE) inhibitor MLN4924 for its effect on GIST cells. Neddylation is an important regulatory process of the proteolytic machinery [25]. It is critical for the recruitment of the E2 ubiquitin-conjugating enzyme to the E3 ligase complex, thereby facilitating ubiquitin conjugation [27]. Inhibition of neddylation therefore inhibits protein degradation by reducing ubiquitination and hence targeting to the proteasome while leaving proteasome function intact. Treatment of GIST cells with increasing concentrations of MLN4924 showed reduction of cellular proliferation starting at 0.1 μM but did not lead to substantial apoptotic activity in luminescence-based assays (Fig. 3D). IC_{50}s ranged from 7.3 μM to 461 μM (Table 1C), favoring IM-resistant cell lines. Results were paralleled on the molecular level by immunoblot analysis (Fig. 3E, Suppl. Fig. 4B). As expected from its mechanism of action, the amount of poly-ubiquitinated proteins decreased with increasing concentrations of MLN4924 (Fig. 3F). This effect started to be seen at fairly low concentrations (0.01 μM) and generally mirrored the cell cycle inhibitory action of the drug (Fig. 3E; Suppl. Fig. 4B).

Taken together, both the DUB inhibitor b-AP15 and the NAE inhibitor MLN4924 only led to minimal pro-apoptotic responses in GIST cells, but MLN4924 showed a prominent cytostatic effect. Interestingly, b-AP15's ability to induce apoptosis and MLN4924's cell cycle inhibitory activity correlated with their ability to modulate ubiquitination and presumably inhibit protein degradation.

Delanzomib, carfilzomib and ixazomib induce GIST cell death by upregulation of H2AX and transcriptional downregulation of KIT

Having shown that the 20S proteasome inhibitors delanzomib, carfilzomib and ixazomib have substantial activity in GIST, we set out to determine the mechanism of action of these compounds. As reported in an earlier study by our group, the prototype proteasome inhibitor bortezomib has a dual mechanism of action in GIST through upregulation of the pro-apoptotic histone H2AX and inhibition of transcription resulting in a dramatic loss of KIT expression [5].

We therefore tested whether delanzomib, carfilzomib and ixazomib have a similar mechanism of action. Indeed, when analyzing H2AX levels by immunoblotting, we found that both phosphorylated and total histone H2AX protein expression increased in a dose- and time-dependent manner (Fig. 4A, B; Suppl. Fig. 5A, B; Suppl. Fig. 6A-D). The increase of phosphorylated and total H2AX levels paralleled the accumulation of ubiquitinated proteins (Fig. 2B, C; Suppl. Fig. 3) and could be demonstrated in both IM-sensitive and IM-resistant GIST cells. In addition, we found that KIT protein expression levels were dramatically downregulated in a dose- and time-dependent manner treatment (Fig.4A, B; Suppl. Fig. 5A, B; Suppl. Fig. 6A-D). As expected, KIT phosphorylation decreased in parallel. To analyze the events that are involved in the downregulation of KIT expression, we examined whether delanzomib leads to transcriptional inhibition of *KIT. KIT* mRNA levels were substantially reduced as shown by RT-PCR (Fig. 4C; Suppl. Methods) and quantitative RT-PCR (qRT-PCR; Fig. 4D; Suppl. Methods). Remarkably, downregulation of *KIT* transcripts was comparable to treatment with bortezomib and the highly effective RNA polymerase II inhibitor α-amanitin (Fig. 4C, D; left panels, GIST882). To determine whether delanzomib affects GIST cell transcription in more general terms, cells were stained for the transcriptional co-activator CREB-binding protein (CBP) by immunofluorescence microscopy (Fig. 4E; Suppl. Fig. 5C; Suppl. Fig. 6E, F; Suppl.

Methods). In DMSO control-treated cells with active transcription, CBP localizes to the transcriptional start sites resulting in a fine-speckled nuclear staining pattern (Fig. 4E; Suppl. Fig. 5C). However, after delanzomib treatment, CBP redistributed into large nuclear displacement foci or was lost completely, indicating a global transcriptional downregulation (Fig. 4E; Suppl. Fig. 5C). Carfilzomib and ixazomib had a similar effect (Suppl. Fig. 6E, F). Transcriptional inhibition after delanzomib treatment was time-dependent over the course of 72 hours. Relocalization of CBP into nuclear foci starts to become apparent at 24 hours, and nuclear protein expression is increasingly lost over the course of the next 48 hours (Suppl. Fig. 7). These results correlate well with our immunoblotting data shown in Fig. 4. While the global transcriptional downregulation that is observed could be worrisome for non-specific toxicity of the compounds tested here, carfilzomib and ixazomib as well as bortezomib are already FDA-approved. The fact that these drugs are safely used in the clinic, therefore speaks against a major impact in patients.

Interestingly, treatment with the DUB inhibitor b-AP15 and the NAE inhibitor MLN4924 also led to increased phosphorylated and total H2AX levels as well as a reduction of total and phosphorylated KIT (Fig. 3B, E; Suppl. Fig. 4). It is of note, that this effect was only seen at the same high drug concentrations that led to an apoptotic response. This is especially striking in case of MLN4924, because its ability to modulate ubiquitination levels and induce cell cycle exit requires much lower drug concentrations (Fig. 3E, F).

Taken together, the pro-apoptotic effect of all compounds targeting the ubiquitin proteasome machinery tested in our study includes a dual mechanism of action resulting in increased levels of soluble histone H2AX and global transcriptional inhibition leading to loss of KIT expression in GIST cells. Nevertheless, there are vast differences in their efficacy with inhibitors of the 20S catalytic core being the most potent compounds. In addition, MLN4924 shows a disconnect between its pro-apoptotic and cell cycle inhibitory

function, the latter of which correlated with the drug's ability to modulate protein ubiquitination.

Delanzomib has* in vivo *antitumor activity in GIST xenografts

Since delanzomib was the strongest inducer of GIST cell death, we next tested its *in vivo* antitumoral activity in several IM-sensitive and IM-resistant GIST xenograft models, including two patient-derived xenografts. Oral treatment with delanzomib led to significant responses in all models tested.

Because of the rapid kinetics seen in our *in vitro* studies, we designed a one-dose bolus experiment, in which mice bearing IM-resistant UZLX-GIST9 patient-derived xenografts received a single dose of oral delanzomib and were sacrificed 24 h later (Suppl. Fig. 8A). While no reduction in tumor size was seen nor expected, histopathologic changes were readily detectable. All treated tumors had a grade 2 or higher histologic response. These changes were accompanied by a significant decrease in the percentage of Ki-67-positive cells as well as a significant increase of cleaved PARP-positive cells (Suppl. Methods). Some tumors already exhibited large areas of central necrosis.

Furthermore, delanzomib resulted in significant tumor reduction comparable to imatinib treatment in the IM-sensitive patient-derived UZLX-GIST1 model over the course of three weeks (Fig. 5A; Suppl. Fig. 8B) [31]. Tumor reduction after delanzomib was accompanied by a marked histopathologic response, and more than 60% of the responses were of grade 3 or higher (Fig. 5B). Response to delanzomib most prominently resulted in large areas of central necrosis, whereas control imatinib treatment rather led to myxoid degeneration, similar to what is seen in clinical imatinib-treated tumor samples [32]. Furthermore, treatment with delanzomib caused a highly significant reduction of proliferation, which was equivalent to imatinib treatment (Fig. 5B). This is exemplified both by reduction of the Ki-67-positive proliferation fraction (from 26.8 % in placebo-treated

controls to 3.0 % in delanzomib-treated tumors) as well as a decrease of mitotic cells positive for phosphorylated histone H3 S10 (from 88/10 HPF in controls to 4/10 HPF in delanzomib-treated tumors; representative areas with higher cellularity depicted in Ki-67/pH3 panels to show loss of expression in comparison to control). Delanzomib also caused increased apoptosis as detected by immunohistochemical staining for cleaved PARP, especially in central areas of the tumor (Fig. 5B; representative areas with central necrosis/myxoid degeneration shown to depict massive cell death). In addition, the percentage of cleaved PARP-positive intratumoral cells increased from 8.9 % in vehicle-treated controls to 15.0 % in delanzomib-treated animals, although not reaching statistical significance. Of note, no increase, but rather a reduced number of cleaved PARP-positive cells was detected in imatinib-treated tumors (1.6 %), indicating that the majority of the remaining tumor cells, while likely not proliferating, could be quiescent [33,34].

The changes described above were also reflected when assessing the response of UZLX-GIST1 to delanzomib (24 h) by immunoblotting (Fig. 5C). While both imatinib- and delanzomib-treated xenografts exhibited reduced cyclin A levels and increased expression of $p27^{Kip1}$ indicating cell cycle arrest, only the delanzomib-treated xenografts showed detectable PARP cleavage. Importantly, delanzomib-treated xenografts also show a downregulation of total KIT protein expression, as would be expected from our *in vitro* data (Fig. 4). Interestingly, a moderate downregulation of KIT resulted in a complete loss of KIT activation. Results were very much comparable to the UZLX-GIST1 bolus treatment as both models already showed drastic changes with respect to induction of apoptosis (PARP cleavage) and reduced cellular proliferation (decreased cyclin A and increased $p27^{Kip1}$ levels in UZLX-GIST1 and decreased Ki-67 expression in UZLX-GIST9) after a single bolus of delanzomib and a short follow-up.

We also tested delanzomib over the course of three weeks in the IM-resistant GIST430 xenograft, where it likewise led to significant histopathologic changes (Fig. 5D).

Sixty percent of the tumors showed a histopathologic response grade of 2 or higher (Suppl. Fig. 8C). Furthermore, treatment with delanzomib caused a highly significant reduction of proliferation, exemplified by the decrease of pH3-positive cells (from 94/10 HPF in controls to 22.5/10 HPF; Fig. 5E; Suppl. Fig. 8D) as well as tumor reduction over time (Suppl. Fig. 8E).

Taken together, delanzomib has significant activity in GIST xenografts, including IM-resistant models.

DISCUSSION

Although GISTs can be successfully treated with tyrosine kinase inhibitors that target KIT, the majority of patients develop resistance to these drugs, mostly through secondary *KIT* mutations. Importantly, these resistance mutations can show significant intertumoral and intratumoral heterogeneity while at the same time conferring sensitivity to different second- or third-line kinase inhibitors. Therefore, therapeutically targeting KIT in a mutation-independent manner is an intriguing strategy.

In the present study, we show that inhibitors of the proteolytic machinery are highly effective in GIST cells and that their mechanism of action is independent of *KIT* mutational status or sensitivity to imatinib. Apoptosis is induced through upregulation of the pro-apoptotic histone H2AX as well as transcriptional downregulation of *KIT*, a mechanism previously described by our group for the first-in-class proteasome inhibitor bortezomib [5–7]. Notably, all tested compounds share this mechanism, regardless of whether they target the 20S proteolytic core of the proteasome or not. The shared transcriptional downregulation of *KIT* raises the possibility that it could be the result of increased H2AX levels, especially in light of the fact that non-chromatin-bound H2AX can lead to

transcriptional inhibition [6]. However, we have shown previously that siRNA-mediated knockdown of H2AX did not completely rescue bortezomib-induced *KIT* transcriptional downregulation, indicating that additional mechanisms are involved [6]. It is well-known that the proteasome has an important role in transcription initiation [35,36]. Transcriptional activation domains of many transcription factors, including ETV1, a main transcription factor of KIT in the GIST/interstitial cell of Cajal lineage [37], often overlap with degrons [35], indicating that their degradation is crucial for transcriptional activation. Similarly, Sp1 is an important transcription factor involved in the regulation of *KIT* [38], and bortezomib has recently been shown to target the specific protein (Sp) family in cancer cells [39]. It therefore seems likely that inhibition of the proteasome directly affects ongoing transcription at the transcription factor level and contributes to the observed transcriptional downregulation of *KIT*.

Although all compounds showed some effect in GIST cells, vast differences in drug efficacy were seen, ranging over three orders of magnitude. Compounds that inhibit the 20S catalytic core of the proteasome (delanzomib, carfilzomib and ixazomib), like bortezomib, stood out as the most potent compounds. Importantly, these second-generation 20S inhibitors have better pharmacologic properties than bortezomib, including an oral route of administration and less toxicity, which warrant their pre-clinical examination without formally determining the clinical utility of bortezomib [15,16,19,30].

Despite being the most active compounds in our study, not all 20S inhibitors were equally effective in GIST cells. In fact, the activity of one compound, delanzomib, was one order of magnitude higher than that of carfilzomib and ixazomib. Delanzomib's IC_{50} was in the low nanomolar range, largely identical to that of bortezomib. Of note, the reason for the superior efficacy of delanzomib does not seem to lie in a structural similarity to bortezomib or its proteasome binding dynamics: Ixazomib – and not delanzomib – is a direct derivative of bortezomib [16,30], and both delanzomib and ixazomib reversibly inhibit

the proteasome, whereas carfilzomib, the least effective 20S inhibitor in our study, inhibits the proteasome irreversibly [13–16,18,19]. Our studies do however point to a similar capability of delanzomib and bortezomib to inhibit the β5 chymotrypsin-like subunit of the proteasome (Fig. 2). In addition, it has recently become clear that co-inhibiting the caspase-like subunit of the proteasome in addition to the chymotrypsin-like subunit increases the ability of proteasome inhibitors to inhibit protein breakdown and enhances their antineoplastic activity [40]. Interestingly, both delanzomib and bortezomib potently inhibit the β1 caspase-like subunit, while carfilzomib and ixazomib do not (15,36). Together, our results indicate that the superior activity of delanzomib is likely mediated through a stronger β5 chymotrypsin-like subunit inhibition and its additional ability to inhibit the β1 caspase-like subunit of the proteasome.

Based on the preclinical results of the compounds tested in our study, delanzomib holds most promise to be effective in the clinical setting for GIST patients. Two early phase clinical trials testing delanzomib in multiple myeloma and solid tumors indeed reported that delanzomib treatment was feasible [20,41]. Importantly, no neurotoxicity, the most severe adverse effect of bortezomib, was reported. While a few partial responses were seen, however, the best result for most delanzomib-treated patients was stable disease [20,41]. Due to the unexpectedly low efficacy, further development of delanzomib for multiple myeloma was discontinued [20].The future of delanzomib as a treatment for GIST is therefore unclear. Nevertheless, testing other 20S proteasome inhibitors could be worthwhile. One possibility could be ixazomib, which has recently been FDA-approved and was the second-most effective drug in our study. Importantly, ixazomib is an orally available drug and would therefore be well-accepted in a patient population that is not otherwise acquainted with intravenously administered medications [16]. In addition, third-generation compounds have become available since we began our study. Especially marizomib (salinosporamide A; Triphase/Celgene), could be of interest because of its

ability to inhibit the β1 caspase-like and β2 trypsin-like subunit in addition to the β5 chymotrypsin-like subunit of the proteasome [42]. As outlined above, this feature seems to be advantageous to ensure a high cytotoxic activity in GIST cells. Marizomib is orally administered and is currently in late phase clinical trials for multiple myeloma, glioma and solid tumors. Another strategy could be to use proteasome inhibitors in combination with other agents, e.g. imatinib. Although preliminary results from our laboratory exploring a combination of imatinib and bortezomib did not show clear synergistic effects, alternative administration regimens, such as drug sequencing, could be explored [43]. Combinations with other agents than imatinib might also be promising. For example, recent strategies combining proteasome inhibitors with other drugs for the treatment of multiple myeloma include AKT/mTOR inhibitors as bortezomib has been shown to increase AKT activation in multiple myeloma cells [44].

Further studies will be needed to delineate why compounds that target other regulators of the proteolytic machinery have a significantly lower efficacy in GIST cells than 20S inhibitors. The DUB inhibitor b-AP15 clearly had a lower ability to induce the accumulation of poly-ubiquitinated proteins and H2AX upregulation as well as transcriptional inhibition of *KIT*. Of note, substantially higher concentrations were also needed to induce ubiquitination in the original report using HCT 116 cells [21]. The *in vivo* efficacy of this compound will therefore depend on its bioavailability and whether it will be feasible to achieve necessary serum levels paired with acceptable toxicity. No clinical trial with b-AP15 has been initiated to this date, but a phase I/II clinical trial to test a derivative, VLX1570 [45], was initiated in 2015 (NCT02372240) and terminated in 2018 due to dose-limiting toxicity (clinicaltrials.gov/ct2/show/NCT02372240).

Our results for the NAE inhibitor MLN4924 are more complex. As mentioned above, this compound inhibits a regulatory mechanism that is critical for facilitating ubiquitin conjugation [25] resulting in decreased ubiquitination and limited protein targeting

to the 26S proteasome [26,27]. The function of the proteasome itself stays intact. MLN4924 exhibited a strong cell cycle inhibitory effect in GIST cells, which correlated well with the expected reduction of ubiquitin-conjugated proteins. The particular effect on the cell cycle can be explained by the fact that neddylation has been specifically implicated in modulating activity of cullin-RING E3 ligases, which control the turnover of cell cycle-regulating proteins, such as $p27^{Kip1}$ [27,28]. It is not that clear why apoptosis is only induced at much higher concentrations of MLN4924, although it did correlate with increased levels of histone H2AX and a decrease in KIT expression, similar to what was seen for the other compounds tested in our study. Although seemingly counterintuitive, both effects can be explained by MLN4924's mechanism of action. As described above, an increase in H2AX levels likely results from decreased degradation due to limited ubiquitination and targeting towards the proteasome. The decrease in KIT expression levels that we observed at high MLN4924 concentrations is likely due to transcriptional inhibition. As mentioned above, it has recently become clear that the ongoing activity of transcriptional activators is dependent on their ubiquitination in addition to the proteolytic capacity of the proteasome [46]. In line with this, MLN4924 has been shown to reduce RNA pol II occupancy at DNA [47]. MLN4924 has moved forward into several clinical studies [48,49]. Nevertheless, the maximal serum concentrations achieved in these trials were lower than the clinically meaningful dose for GIST patients and confirms that MLN4924 is not a medication to move forward in this entity.

Unfortunately, many preclinical studies never reach clinical success. While the ultimate significance of proteasome inhibitors for the treatment of patients with GIST is difficult to estimate, the fact that our *in vitro* and *in vivo* results are similar to what has been reported in multiple myeloma models is promising. For example, treatment of bortezomib-sensitive multiple myeloma (MM) cell lines with delanzomib and bortezomib at concentrations comparable to what we used in our study had a similar effect with respect

to the accumulation of ubiquitinated proteins [18]. Another important question for preclinical studies is whether the concentration at which the biologic effects occur are achievable in the serum. Delanzomib serum concentrations for multiple myeloma, for example, while lower than the calculated effective serum concentration needed to treat GIST patients, showed high peak concentrations after initial administration with a rapid distribution into the extra-vascular space [41]. Paired with a prolonged elimination phase and a mean half-life of 62 hours, drug concentrations in the tumor could therefore be sufficient for exerting a biological effect. Similarly, our preclinical data for ixazomib are not that different from what has been reported for myeloma models [30]. On the other hand, it might be difficult to achieve effective serum concentrations of carfilzomib in the patient setting.

In summary, we have shown that inhibitors of the ubiquitin-proteasome machinery, especially those that inhibit the 20S proteolytic core, have therapeutic activity in imatinib-sensitive and imatinib-resistant GIST model systems. Clinical studies are encouraged.

MATERIALS AND METHODS

Cell culture and inhibitor treatments

An array of imatinib (IM)-sensitive and IM-resistant human GIST cell lines was used in the present study. IM-sensitive cells included GIST882 (kindly provided by Jonathan A. Fletcher, Brigham and Women's Hospital, Boston, MA, USA) and GIST-T1 (kindly provided by Takahiro Taguchi, Kochi Medical School, Nankoku Kochi, Japan) [50]. As described previously, GIST882 cells carry a homozygous mutation in *KIT* exon 13 (p.K642E) and GIST-T1 cells are characterized by a heterozygous *KIT* exon 11 deletion (p.V560_Y578del) [50]. The IM-resistant GIST cell lines GIST430 (heterozygous *KIT* exon 11 deletion, p.V560_L576del; *KIT* exon 13 point mutation, p.V654A) and GIST48

(homozygous *KIT* exon 11 mutation, p.V560D; *KIT* exon 17 point mutation, p.D820A) were derived from human GISTs that developed clinical resistance to IM therapy (J.A. Fletcher) [51]. Cells were maintained as described previously [51].

Cells were treated with carfilzomib (CFZ, Fisher), ixazomib (IXA, SelleckChem), delanzomib (DLZ, SelleckChem, Toronto Research Chemicals), b-AP15 (EMD Millipore) or MLN-4924 (SelleckChem) at the indicated concentrations in DMSO or mock-treated with 0.1% DMSO for up to 72 h, as indicated. Treatment with imatinib mesylate (1 µM in DMSO; LC Laboratories), sunitinib malate (1 µM in DMSO; LC Laboratories), bortezomib (0.01 µM in DMSO; LC Laboratories) as well as α-amanitin (1µg/mL in dH_2O; Sigma) served as controls.

Antibodies

Primary antibodies used for immunoblotting, immunofluorescence and immunohistochemistry were actin (Sigma), cleaved caspase 3 (Cell Signaling), CREB binding protein (CBP; Santa Cruz), cyclin A (Novocastra), pH2AX S139 (Millipore), H2AX (Bethyl), phospho-histone H3 S10, phospho-KIT Y719 (both Cell Signaling), Ki-67 (Thermo Scientific Neomarkers), KIT (Dako/Agilent), $p27^{Kip1}$ (Fisher/BD Biosciences Pharmingen), PARP (Invitrogen), cleaved PARP (Abcam) and mono-ubiquitin (BD Pharmingen).

26S proteasome activity assay

The chymotrypsin-like activity of the proteasome after treatment with the above-mentioned proteasome inhibitors was measured using the luminescence-based Proteasome-Glo assay (Promega). Cells were plated in 96-well flat-bottomed plates (Perkin Elmer), cultured for 24 h and then incubated for 2 h with the respective compounds at indicated concentrations or DMSO-only solvent control. A peptide substrate for the

chymotrypsin-like activity of the proteasome conjugated to recombinant luciferase, Suc-LLVY-(succinyl-leucine-leucine-valine-tyrosine-)aminoluciferin, was added for 10 minutes, before luminescence was measured with a BioTek Synergy 2 Luminometer (BioTek). Data were normalized to the DMSO-only control group.

GIST xenograft models

In vivo studies were carried out at the Laboratory of Experimental Oncology, KU Leuven (Leuven, Belgium) according to local guidelines and Belgian regulations and were approved by the Ethical Committee for Laboratory Animal Research, KU Leuven. UZLX-GIST1 (IM-sensitive; *KIT* exon 11 mutation, p.V560D) and UZLX-GIST9 (IM-resistant) were derived from clinical samples of consenting GIST patients treated at the University Hospitals Leuven, as previously described [52,53]. UZLX-GIST9 initially presented with a primary *KIT* exon 11 p.P577del mutation. At time of metastasis, mutational analysis revealed the original mutation as well as a *KIT* exon 11 frameshift (p.W557LfsX5) and a *KIT* exon 13 point mutation (p.D820G) [52]. UZLX-GIST1 (passage 23), UZLX-GIST9 (passage12) and GIST430 (passage 6) xenografts were created by bilateral transplantation of tumor fragments into the flank of female adult athymic nude mice (NMRI, nu/nu; Janvier Laboratories). When tumors were 1 cm in diameter, mice were randomized into groups of 4-6 animals each for different treatment regimens. Delanzomib (in 5% mannitol: propylene glycol [4:1 v/v]) was administered by oral gavage twice a week for three weeks. Imatinib-treated mice (50 mg/kg twice a day, p.o.) served as positive control, while mice receiving vehicle were used as negative control. A maximum-tolerated dose experiment for delanzomib using 6 *vs.* 8 mg/kg was conducted. All mice tolerated the higher dose of 8 mg/kg well (data not shown), which was used in all experiments. Above doses were chosen according to the literature, where oral dosing between 7.8 mg/kg and 13 mg/kg was tested in myeloma models [18,54]. Our selected dose of 8 mg/kg was at the

low end of the spectrum for myeloma studies and should hence well translate into the human setting. Tumor volume, weight and general health of the mice were recorded [52]. After the mice were sacrificed, tumors were excised and divided for fresh frozen samples and histopathologic examination. Histopathologic grading of the response to the compounds was based on the microscopic amount of necrosis, myxoid degeneration or fibrosis with grade 1 representing a minimal response (0-10%) and grade 4 representing a maximal response (>90%) [55].

Statistics

Statistical significance was assessed using Student's t test for independent samples. *P* values ≤0.05 were considered significant.

DATA AVAILABILITY

The data set generated during and/or analyzed during the current study are available from the corresponding author on reasonable request.

REFERENCES

1. Verweij, J. *et al.* Progression-free survival in gastrointestinal stromal tumours with high-dose imatinib: randomised trial. *Lancet* **364**, 1127–1134 (2004).
2. Gramza, A. W., Corless, C. L. & Heinrich, M. C. Resistance to Tyrosine Kinase Inhibitors in Gastrointestinal Stromal Tumors. *Clin Cancer Res* **15**, 7510–7518 (2009).
3. Voges, D., Zwickl, P. & Baumeister, W. The 26S proteasome: A molecular machine designed for controlled proteolysis. *Annu Rev Biochem* **68**, 1015–1068 (1999).
4. Manasanch, E. E. & Orlowski, R. Z. Proteasome inhibitors in cancer therapy. *Nat. Rev. Clin. Oncol.* **14** 417–433 (2017).
5. Bauer, S. *et al.* Proapoptotic activity of bortezomib in gastrointestinal stromal tumor cells. *Cancer Res.* **70**, 150–159 (2010).
6. Liu, Y. *et al.* Histone H2AX is a mediator of gastrointestinal stromal tumor cell apoptosis following treatment with imatinib mesylate. *Cancer Res.* **67**, 2685–2692 (2007).
7. Liu, Y., Parry, J. A. J. A., Chin, A., Duensing, S. & Duensing, A. Soluble histone H2AX is induced by DNA replication stress and sensitizes cells to undergo apoptosis. *Mol. Cancer* **7**, 61 (2008).
8. Rausch, J. L. *et al.* Opposing roles of KIT and ABL1 in the therapeutic response of gastrointestinal stromal tumor (GIST) cells to imatinib mesylate. *Oncotarget* **8**, 4471–4483 (2017).
9. Maki, R. G. *et al.* A multicenter Phase II study of bortezomib in recurrent or metastatic sarcomas. *Cancer* **103**, 1431–1438 (2005).
10. Bahleda, R. *et al.* Phase I trial of bortezomib daily dose: safety, pharmacokinetic profile, biological effects and early clinical evaluation in patients with advanced solid tumors. *Invest. New Drugs* **36**, 619-628 (2019).
11. Deming, D. A. *et al.* A Phase I study of intermittently dosed vorinostat in combination with bortezomib in patients with advanced solid tumors. *Invest. New Drugs* **32**, 323–329 (2013).
12. Papandreou, C. N. *et al.* Phase I Trial of the Proteasome Inhibitor Bortezomib in Patients With Advanced Solid Tumors With Observations in Androgen-Independent Prostate Cancer. *J. Clin. Oncol.* **22**, 2108–2121 (2004).
13. Demo, S. D. *et al.* Antitumor activity of PR-171, a novel irreversible inhibitor of the proteasome. *Cancer Res.* **67**, 6383–6391 (2007).
14. Herndon, T. M. *et al.* U.s. Food and Drug Administration approval: carfilzomib for the treatment of multiple myeloma. *Clin Cancer Res* **19**, 4559–4563 (2013).
15. O'Connor, O. A. *et al.* A phase 1 dose escalation study of the safety and pharmacokinetics of the novel proteasome inhibitor carfilzomib (PR-171) in patients with hematologic malignancies. *Clin Cancer Res* **15**, 7085–7091 (2009).
16. Kupperman, E. *et al.* Evaluation of the proteasome inhibitor MLN9708 in preclinical models of human cancer. *Cancer Res.* **70**, 1970–1980 (2010).

17. Shirley, M. Ixazomib: First Global Approval. *Drugs* **76**, 405–411 (2016).

18. Piva, R. *et al.* CEP-18770: A novel, orally active proteasome inhibitor with a tumor-selective pharmacologic profile competitive with bortezomib. *Blood* **111**, 2765–2775 (2008).

19. Dorsey, B. D. *et al.* Discovery of a potent, selective, and orally active proteasome inhibitor for the treatment of cancer. *J. Med. Chem.* **51**, 1068–1072 (2008).

20. Vogl, D. T. *et al.* Phase I/II study of the novel proteasome inhibitor delanzomib (CEP-18770) for relapsed and refractory multiple myeloma. *Leuk. & Lymphoma* **58**, 1872–1879 (2016).

21. D'Arcy, P. aacute draig *et al.* Inhibition of proteasome deubiquitinating activity as a new cancer therapy. *Nat. Med.* **17**, 1636–1640 (2011).

22. Oh, Y.-T., Deng, L., Deng, J. & Sun, S.-Y. The proteasome deubiquitinase inhibitor b-AP15 enhances DR5 activation-induced apoptosis through stabilizing DR5. *Sci. Rep.* **7**, 8027 (2017). doi:10.1038/s41598-017-08424-w

23. Tian, Z. *et al.* A novel small molecule inhibitor of deubiquitylating enzyme USP14 and UCHL5 induces apoptosis in multiple myeloma and overcomes bortezomib resistance. *Blood* **123**, 706–716 (2014).

24. Chitta, K. *et al.* Targeted inhibition of the deubiquitinating enzymes, USP14 and UCHL5, induces proteotoxic stress and apoptosis in Waldenström macroglobulinaemia tumour cells. *Br. J. Haematol.* **169**, 377–390 (2015).

25. Kumar, S., Yoshida, Y. & Noda, M. Cloning of a cDNA Which Encodes a Novel Ubiquitin-like Protein. *Biochem. Biophys. Res. Commun.* **195**, 393–399 (1993).

26. Hori, T. *et al.* Covalent modification of all members of human cullin family proteins by NEDD8. *Oncogene* **18**, 6829–6834 (1999).

27. Soucy, T. A., Dick, L. R., Smith, P. G., Milhollen, M. A. & Brownell, J. E. The NEDD8 conjugation pathway and its relevance in cancer biology and therapy. *Genes & Cancer* **1**, 708–716 (2010).

28. Soucy, T. A. *et al.* An inhibitor of NEDD8-activating enzyme as a new approach to treat cancer. *Nature* **458**, 732–736 (2009).

29. Chauhan, D. *et al.* A small molecule inhibitor of ubiquitin-specific protease-7 induces apoptosis in multiple myeloma cells and overcomes bortezomib resistance. *Cancer Cell* **22**, 345–358 (2012).

30. Chauhan, D. *et al.* In vitro and in vivo selective antitumor activity of a novel orally bioavailable proteasome inhibitor MLN9708 against multiple myeloma cells. *Clin Cancer Res* **17**, 5311–5321 (2011).

31. Li, H. *et al.* Pazopanib, a Receptor Tyrosine Kinase Inhibitor, Suppresses Tumor Growth through Angiogenesis in Dedifferentiated Liposarcoma Xenograft Models. *Transl. Oncol.* **7**, 665–671 (2014).

32. Floris, G. *et al.* High Efficacy of Panobinostat Towards Human Gastrointestinal Stromal Tumors in a Xenograft Mouse Model. *Clin. Cancer Res.* **15**, 4066–4076 (2009).

33. Liu, Y. *et al.* Imatinib mesylate induces quiescence in gastrointestinal stromal tumor cells through the CDH1-SKP2-p27Kip1 signaling axis. *Cancer Res.* **68**, 9015–9023

(2008).

34. Boichuk, S. *et al.* The DREAM complex mediates GIST cell quiescence and is a novel therapeutic target to enhance imatinib-induced apoptosis. *Cancer Res.* **73**, 5120–5129 (2013).

35. Geng, F., Wenzel, S. & Tansey, W. P. Ubiquitin and Proteasomes in Transcription. *Annu Rev Biochem* **81**, 177–201 (2012).

36. Durairaj, G. & Kaiser, P. The 26S Proteasome and Initiation of Gene Transcription. *Biomolecules* **4**, 827–847 (2014).

37. Chi, P. *et al.* ETV1 is a lineage survival factor that cooperates with KIT in gastrointestinal stromal tumours. *Nature* **467**, 849–853 (2010).

38. Park, G. H., Plummer, H. K. & Krystal, G. W. Selective Sp1 binding is critical for maximal activity of the human c-kit promoter. *Blood* **92**, 4138–4149 (1998).

39. Karki, K., Harishchandra, S. & Safe, S. Bortezomib Targets Sp Transcription Factors in Cancer Cells. *Mol. Pharmacol.* **94**, 1187–1196 (2018).

40. Britton, M. *et al.* Selective Inhibitor of Proteasome□s Caspase-like Sites Sensitizes Cells to Specific Inhibition of Chymotrypsin-like Sites. *Chem. Biol.* **16**, 1278–1289 (2009).

41. Gallerani, E. *et al.* A first in human phase I study of the proteasome inhibitor CEP-18770 in patients with advanced solid tumours and multiple myeloma. *Eur J Cancer* **49**, 290–296 (2013).

42. Chauhan, D. *et al.* A novel orally active proteasome inhibitor induces apoptosis in multiple myeloma cells with mechanisms distinct from Bortezomib. *Cancer Cell* **8**, 407–419 (2005).

43. Serrano, C. *et al.* Complementary activity of tyrosine kinase inhibitors against secondary kit mutations in imatinib-resistant gastrointestinal stromal tumours. *Br. J. Cancer* **120**, (2019).

44. Kapoor, P., Ramakrishnan, V. & Rajkumar, S. V. Bortezomib Combination Therapy in Multiple Myeloma. *Semin. Hematol.* **49**, 228–242 (2012).

45. Wang, X. *et al.* The proteasome deubiquitinase inhibitor VLX1570 shows selectivity for ubiquitin-specific protease-14 and induces apoptosis of multiple myeloma cells. *Sci. Rep.* **6**, 26979 (2016).

46. Lipford, J. R. & Deshaies, R. J. Diverse roles for ubiquitin-dependent proteolysis in transcriptional activation. *Nat. Cell Biol.* **5**, 845–850 (2003).

47. Chen, C. P. *et al.* Kaposi's Sarcoma-Associated Herpesvirus Hijacks RNA Polymerase II To Create a Viral Transcriptional Factory. *J. Virol.* **91**, e02491-16–17 (2017).

48. Shah, J. J. *et al.* Phase I Study of the Novel Investigational NEDD8-Activating Enzyme Inhibitor Pevonedistat (MLN4924) in Patients with Relapsed/Refractory Multiple Myeloma or Lymphoma. *Clin Cancer Res* **22**, 34–43 (2016).

49. Bhatia, S. *et al.* A phase I study of the investigational NEDD8-activating enzyme inhibitor pevonedistat (TAK-924/MLN4924) in patients with metastatic melanoma. *Invest. New Drugs* **34**, 439–449 (2016).

50. Taguchi, T. *et al.* Conventional and molecular cytogenetic characterization of a new

human cell line, GIST-T1, established from gastrointestinal stromal tumor. *Lab. Invest.* **82**, 663–665 (2002).

51. Boichuk, S. *et al.* Unbiased compound screening identifies unexpected drug sensitivities and novel treatment options for gastrointestinal stromal tumors. *Cancer Res.* **74**, 1200–1213 (2014).

52. Van Looy, T. *et al.* Characterization and assessment of the sensitivity and resistance of a newly established human gastrointestinal stromal tumour xenograft model to treatment with tyrosine kinase inhibitors. *Clin. Sarcoma Res.* **4**, 10 (2014).

53. Van Looy, T. *et al.* Therapeutic Efficacy Assessment of CK6, a Monoclonal KIT Antibody, in a Panel of Gastrointestinal Stromal Tumor Xenograft Models. *Transl. Oncol.* **8**, 112–118 (2015).

54. Sanchez, E. *et al.* The proteasome inhibitor CEP-18770 enhances the anti-myeloma activity of bortezomib and melphalan. *Br. J. Haematol.* **148**, 569–581 (2010).

55. Agaram, N. P. *et al.* Pathologic and molecular heterogeneity in imatinib-stable or imatinib-responsive gastrointestinal stromal tumors. *Clin Cancer Res* **13**, 170–181 (2007).

ACKNOWLEDGEMENTS

The authors would like to thank Jonathan A. Fletcher and Takahiro Taguchi for sharing important reagents, Sarangarajan Ranganathan and Ivy John for expertise in mouse histopathology, Jennifer D. Francis, Laura Presutti, Eric W. Weil and Michelle Wolf for technical assistance as well as Stefan Duensing for critically reading the manuscript and helpful discussions. This work was supported by a Research Scholar Grant from the American Cancer Society (RSG-08-092-01-CCG; to A.D), the GIST Cancer Research Fund (to A.D.), The Life Raft Group (to A.D. and M.D.R.), the Out of the Woods Foundation (to A.D.), the Flemish Cancer Society (to P.S.) and numerous private donations (to A.D.). A.D. is supported by the UPMC Hillman Cancer Center and in part by a grant from the Pennsylvania Department of Health. The Department specifically disclaims responsibility for any analyses, interpretations or conclusions.

AUTHOR CONTRIBUTIONS

Conception and design: AD. Development of methodology: JLR, AAA, KRMe, KRMa, MDR, AW, AD. Acquisition of data: JLR, AAA, DML, YKG, KRMe, AA, SSP, YT, JW, HSD, MDR, AW, AD. Analysis and interpretation of data: JLR, AAA, DML, KRMe, AA, SSP, AW, AD. Writing, review and/or revision of the manuscript: JLR, DML, SSP, MDR, AW, AD. Administrative, technical, or material support: KRMa, PS, MDR, AD. Study supervision: AD.

COMPETING INTEREST

The authors declare no competing interests.

FIGURE LEGENDS

Figure 1. The second-generation inhibitors of the 26S proteasome delanzomib (DLZ), carfilzomib (CFZ) and ixazomib (IXA) effectively induce cell cycle arrest and apoptosis in imatinib (IM)-sensitive and IM-resistant GIST cells.

(A, B) Dose-dependent effect of delanzomib, carfilzomib and ixazomib in comparison to bortezomib (BO) on cell viability **(A)** and induction of apoptosis **(B)** of imatinib (IM)-sensitive (GIST882, GIST-T1) and IM-resistant (GIST48, GIST430) GIST cells as measured by luminescence-based assays (mean +/- SE).

(C, D) Immunoblot analysis for markers of cell cycle regulation and apoptosis after treatment of GIST cells with increasing concentrations (0.0001 μM – 10 μM; 72 h) of delanzomib **(C)**, carfilzomib **(D,** top panels**)** or ixazomib **(D,** bottom panels**)**. Treatment with IM (1.0 μM), sunitinib (SU; 1.0 μM) or BO (0.1 μM) serves as positive control.

(E) Dose-dependent effect of delanzomib on induction of apoptosis in GIST882 and GIST48 cells as measured by TUNEL assay. Cells were treated for 72 h. Graphs represent mean and standard error of at least three experiments with at least 100 cells counted each. Scale bars, 50 μm (left panels); 20 μm (right panels). *, $p \leq 0.05$ in comparison to control; **, $p \leq 0.01$ in comparison to control; ***, $p \leq 0.001$ in comparison to control (Student's t-test, 2-tailed).

(F) Immunoblot analysis for markers of cell cycle regulation and apoptosis after treatment of GIST cells with DMSO or delanzomib (0.1 μM) for the indicated times.

(C, D, F) Grouped immunoblot images are either cropped from different parts of the same gel or from a separate gel run with another aliquot of the same protein lysate.

Figure 2. Delanzomib (DLZ), carfilzomib (CFZ) and ixazomib (IXA) strongly inhibit the activity of the 26S proteasome and rapidly lead to the accumulation of ubiquitinated proteins.

(A) Dose-dependent effect of delanzomib, carfilzomib and ixazomib on the activity of the 26S proteasome in GIST cells. Cells were treated with increasing concentrations of delanzomib (0.0001 µM to 10 µM) for 2 h, and 26S proteasome activity was determined using a luminescence-based assay.

(B, C) Dose- **(B)** and time-dependent **(C)** accumulation of mono-ubiquitinated proteins in GIST cells after delanzomib treatment as determined by immunoblotting. As expected, kinase inhibitor treatment with IM or SU (both 1.0 µM; 72 h) did not lead to increased ubiquitination.

Figure 3. **The USP14/UCHL5 inhibitor b-AP15 and the NEDD8 inhibitor MLN4924 are only effective at high concentrations or have a mostly cytostatic effect in GIST cells.**

(A) Dose-dependent effect of b-AP15 on cell viability (left) and induction of apoptosis (right) of IM-sensitive (GIST882, GIST-T1) and IM-resistant (GIST48, GIST430) GIST cells as measured by luminescence-based assays (mean +/- SE). The abrupt drop of caspase 3/7 activity in IM-resistant cells treated with 10 µM b-AP15 most likely indicates that the majority of cells were killed and that b-AP15 was extremely effective in these cells at this high concentration.

(B, C) Immunoblot analysis for markers of cell cycle regulation and apoptosis **(B)** and accumulation of mono-ubiquitinated proteins **(C)** in GIST cells after treatment with increasing concentrations (0.0001 µM – 10 µM; 72 h) of b-AP15. Treatment with IM or SU (both 1.0 µM) serves as control.

(D) Dose-dependent effect of MLN4924 on cell viability (left) and induction of apoptosis (right) of GIST cells as measured by luminescence-based assays (mean +/- SE).

(E, F) Immunoblot analysis for markers of cell cycle regulation and apoptosis **(E)** and accumulation of mono-ubiquitinated proteins **(F)** after treatment with increasing concentrations (0.0001 µM – 10 µM; 72 h) of MLN4924. Treatment with IM, SU (both 1.0 µM) or BO (0.1 µM) serves as control.

(B, E) Grouped immunoblot images are either cropped from different parts of the same gel or from a separate gel run with another aliquot of the same protein lysate.

Figure 4. Delanzomib (DLZ) treatment leads to upregulation of soluble histone H2AX, but downregulates KIT expression through inhibition of transcription, similar to bortezomib.

(A, B) Immunoblot analysis of GIST cells treated with delanzomib at the indicated concentrations for 72 h **(A)** or with 0.1 µM delanzomib for the indicated times **(B)** and probed for phospho-H2AX (S139) and total H2AX as well as phospho-KIT (Y719) and total KIT. Grouped immunoblot images are either cropped from different parts of the same gel or from a separate gel run with another aliquot of the same protein lysate.

(C, D) RT-PCR **(C)** and quantitative RT-PCR (qRT-PCR) amplification **(D)** of *KIT* mRNA after treating GIST cells with DMSO or 0.1 µM delanzomib in comparison to bortezomib (BO) for 48 h. GIST882 cells were also treated with the RNA polymerase II inhibitor α-amanitin (α -ama) or H_2O solvent control.

(E) Immunofluorescence microscopic analysis of GIST882 and GIST48 cells treated with DMSO or 0.1 µM delanzomib for 72 h and stained for the transcriptional co-activator CREB-binding protein (CBP; green). Nuclei were stained with DAPI. Bar, 20 µm.

Figure 5. Delanzomib has *in vivo* antitumor activity in IM-sensitive and IM-resistant GIST xenografts.

(A) Relative tumor volume of UZLX-GIST1 xenografts over the course of a 21-day treatment with vehicle, delanzomib or imatinib. Averages represent the average of at least four tumors per group.

(B) Histopathologic response of imatinib-sensitive UZLX-GIST1 xenografts to treatment with delanzomib in comparison with placebo-treated and imatinib-treated positive control. Hematoxylin and eosin (H&E) as well as immunohistochemical staining for Ki-67, phosphorylated histone H3 S10 or cleaved PARP (10X magnification). Histopathologic response grade was determined according to Agaram et al. [55]. Data shown in graph represent at least six tumors per group. Quantification of proliferation index (% Ki-67 positive cells), mitotic cells (pH3-positive cells per 10 HPF) and percentage of cleaved PARP-positive cells (brown staining, respectively) represents the average of at least six tumors per group. Columns, mean + SE; *, $p \leq 0.05$ in comparison to control; **, $p \leq 0.01$ in comparison to control; ***, $p \leq 0.001$ in comparison to control (Student's t-test, 2-tailed).

(C) Immunoblot analysis of UZLX-GIST1 xenografts treated with delanzomib (24 h) in comparison with placebo treatment and imatinib-treated positive control. Each lane represents one xenograft (C, vehicle control; DLZ, delanzomib; IM, imatinib). Grouped immunoblot images are either cropped from different parts of the same gel or from a separate gel run with another aliquot of the same protein lysate.

(D) Histopathologic response of imatinib-resistant GIST430 xenografts to treatment with delanzomib in comparison with placebo.

(E) Immunohistochemical staining for phosphorylated histone H3 S10 in GIST430 xenografts treated with delanzomib or placebo control.

TABLES

Table 1. IC_{50} and EC_{50} values of compounds affecting the ubiquitin proteasome machinery in imatinib (IM)-sensitive and IM-resistant GIST cells. (A) IC_{50} (cell viability) of carfilzomib (CFZ), ixazomib (IXA) and delanzomib (DLZ) in comparison to bortezomib (BO). (B) EC_{50}s of 20S inhibition of carfilzomib (CFZ), ixazomib (IXA) and delanzomib (DLZ) in comparison to bortezomib (BO). (C) IC_{50}s (cell viability) of the USP14/UCHL5 inhibitor b-AP15 and the NEDD8 activating enzyme inhibitor MLN4924. IM-sensitive: GIST882, GIST-T1; IM-resistant: GIST48, GIST430.

(A)

	IC_{50} (nM)			
	CFZ	IXA	DLZ	BO
GIST882	184	82	23	13
GIST-T1	1,679	175	36	26
GIST48	67	41	9	7
GIST430	185	56	12	13

(B)

	EC_{50} (nM)			
	CFZ	IXA	DLZ	BO
GIST882	96	84	13	8
GIST-T1	41	50	5	9
GIST48	52	25	7	6
GIST430	83	42	5	4

(C)

	IC_{50} (nM)	
	b-AP15	**MLN4924**
GIST882	>10,000	>10,000
GIST-T1	**>10,000**	**>10,000**
GIST48	473	7,333
GIST430	**1,219**	**>10,000**

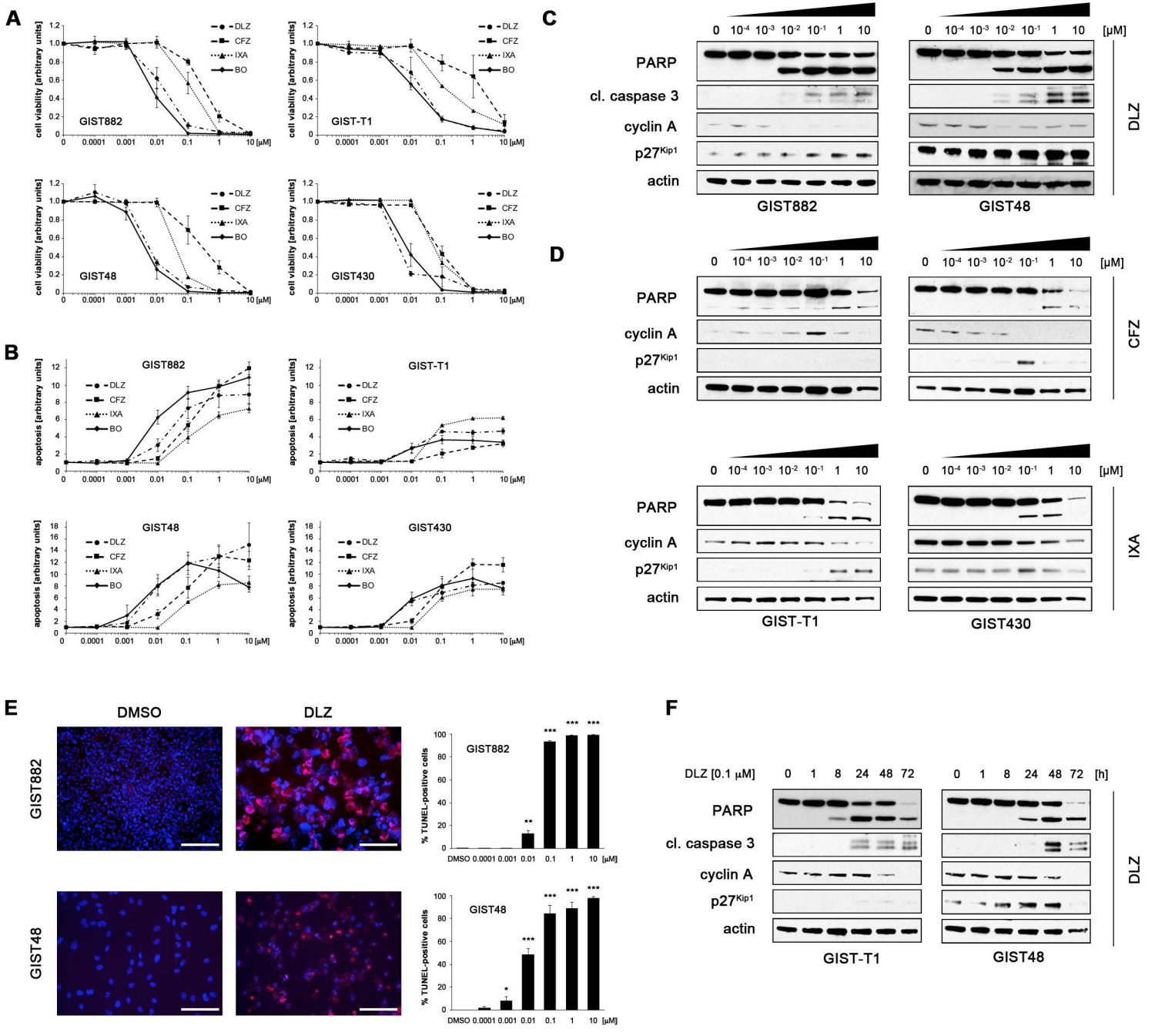

Rausch *et al.*, Figure 1

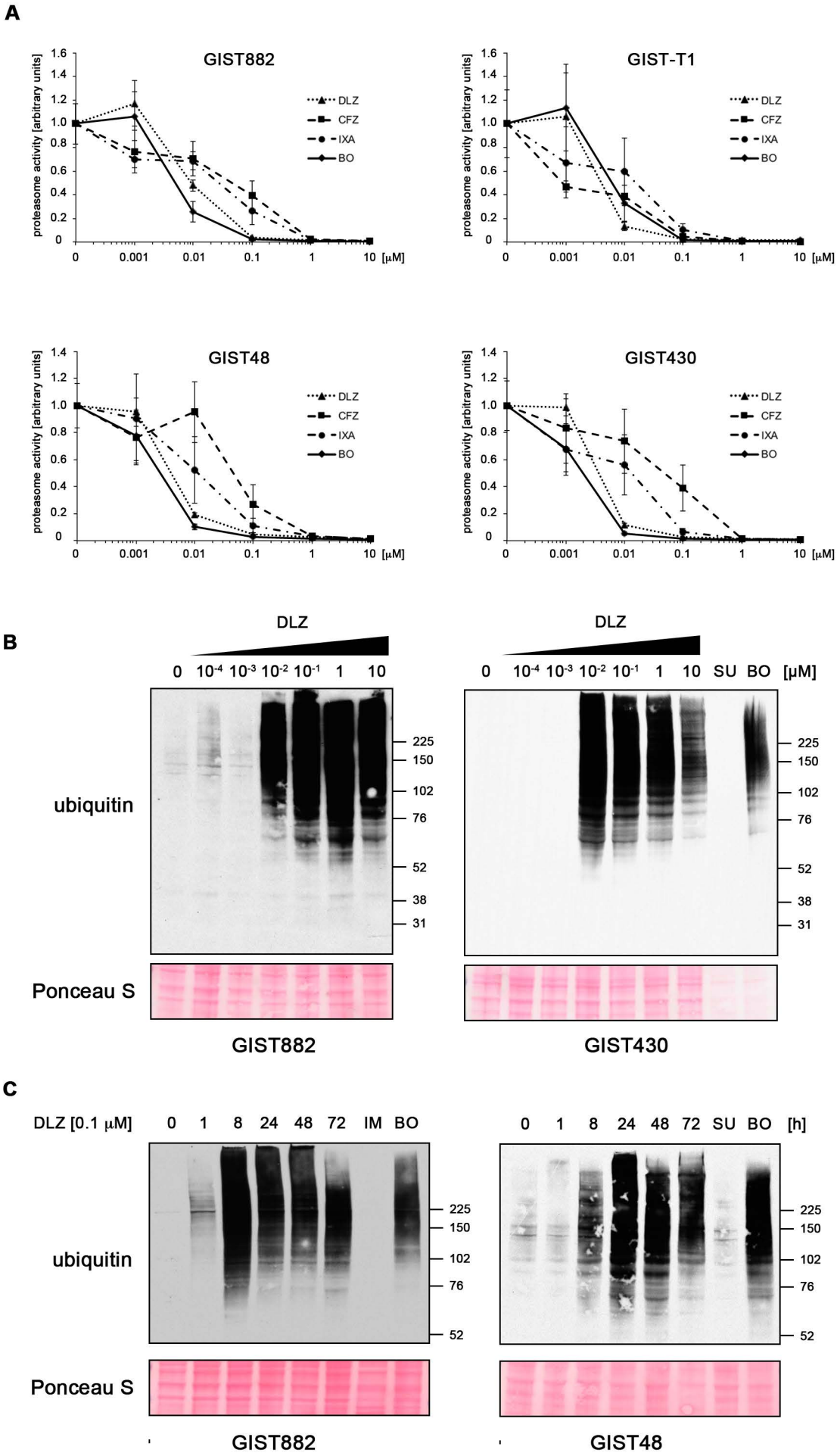

Rausch *et al.*, Figure 2

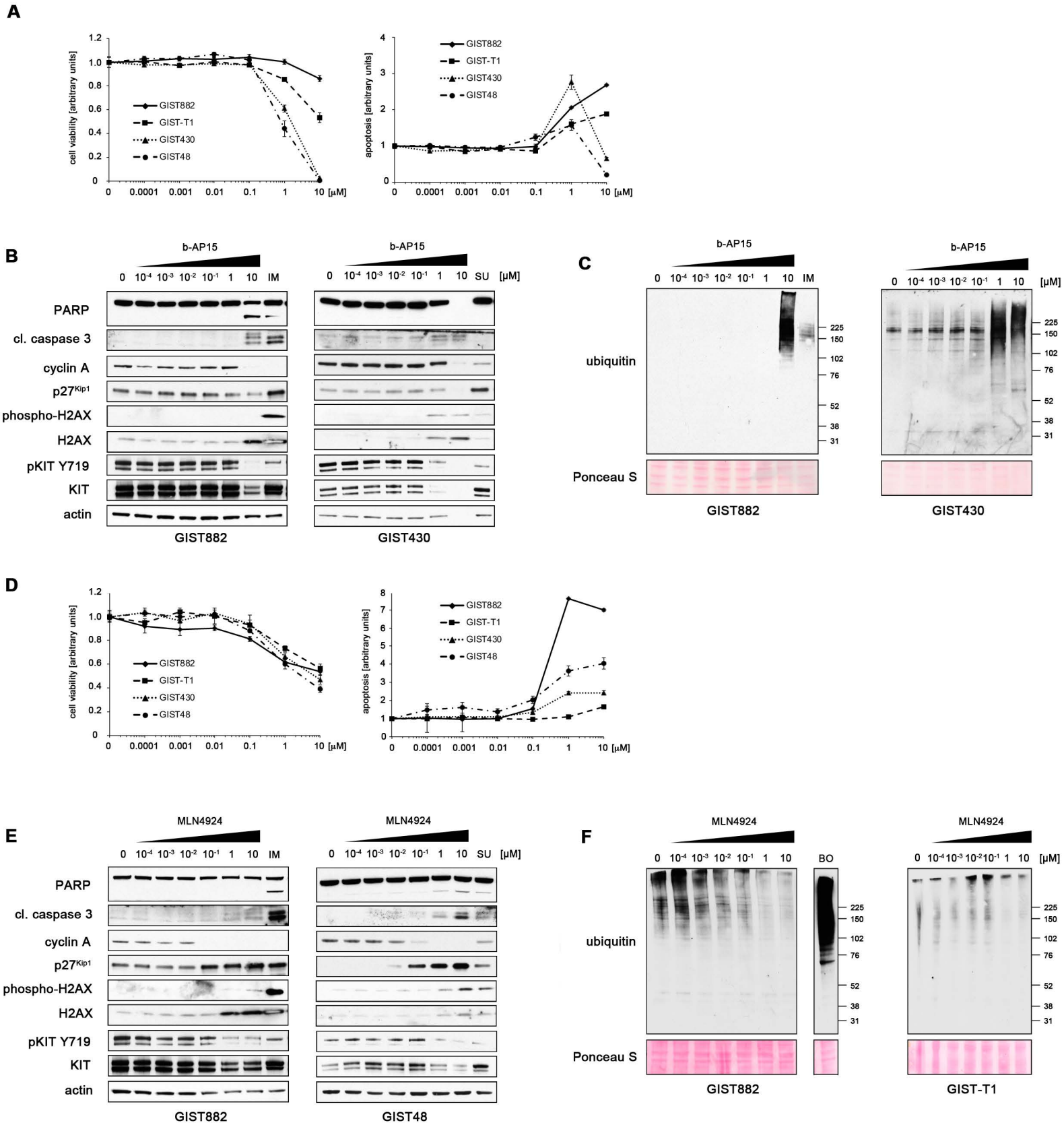

Rausch *et al.*, Figure 3

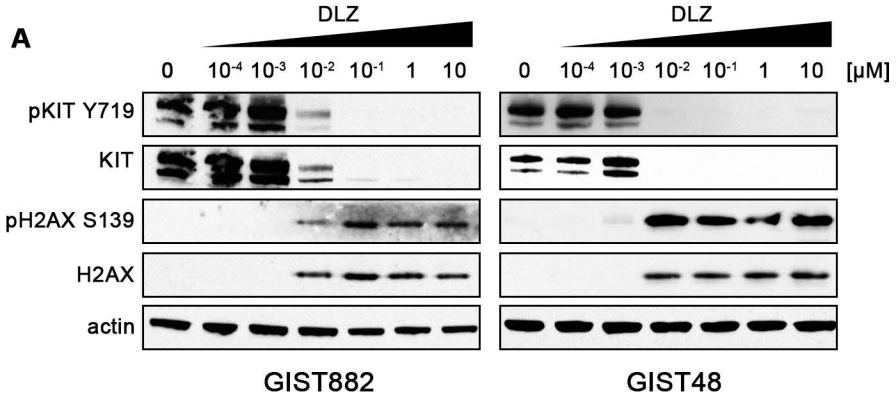

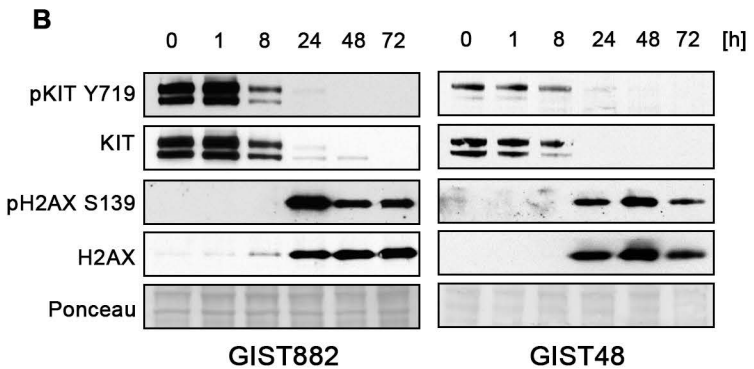

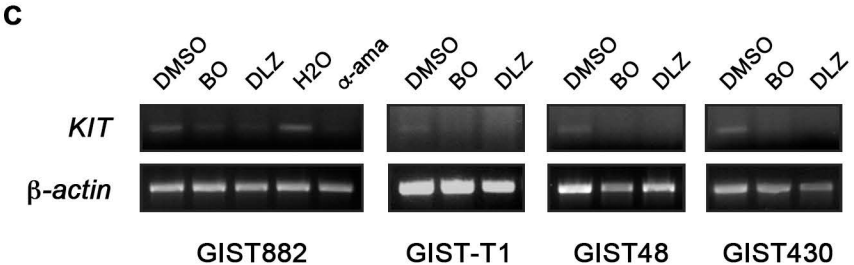

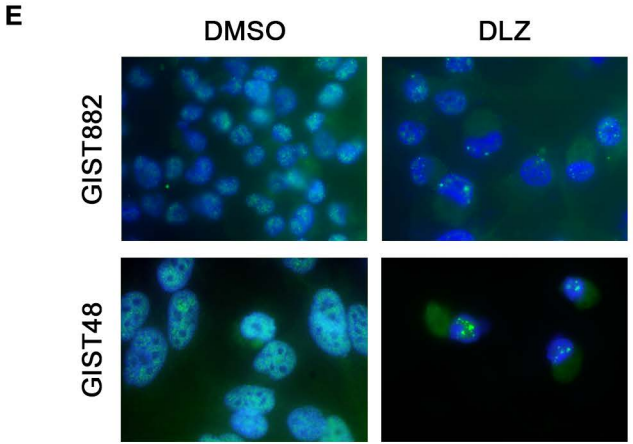

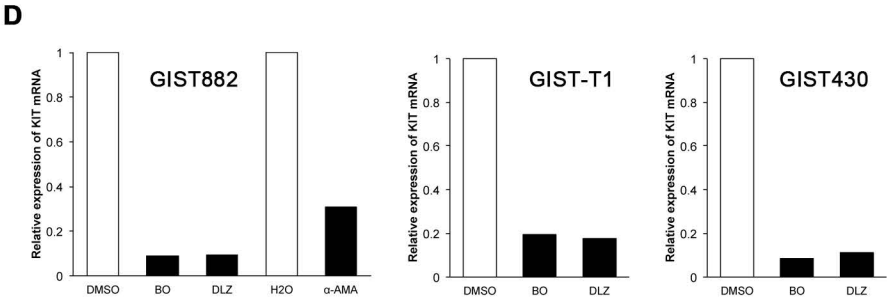

Rausch *et al.*, Figure 4

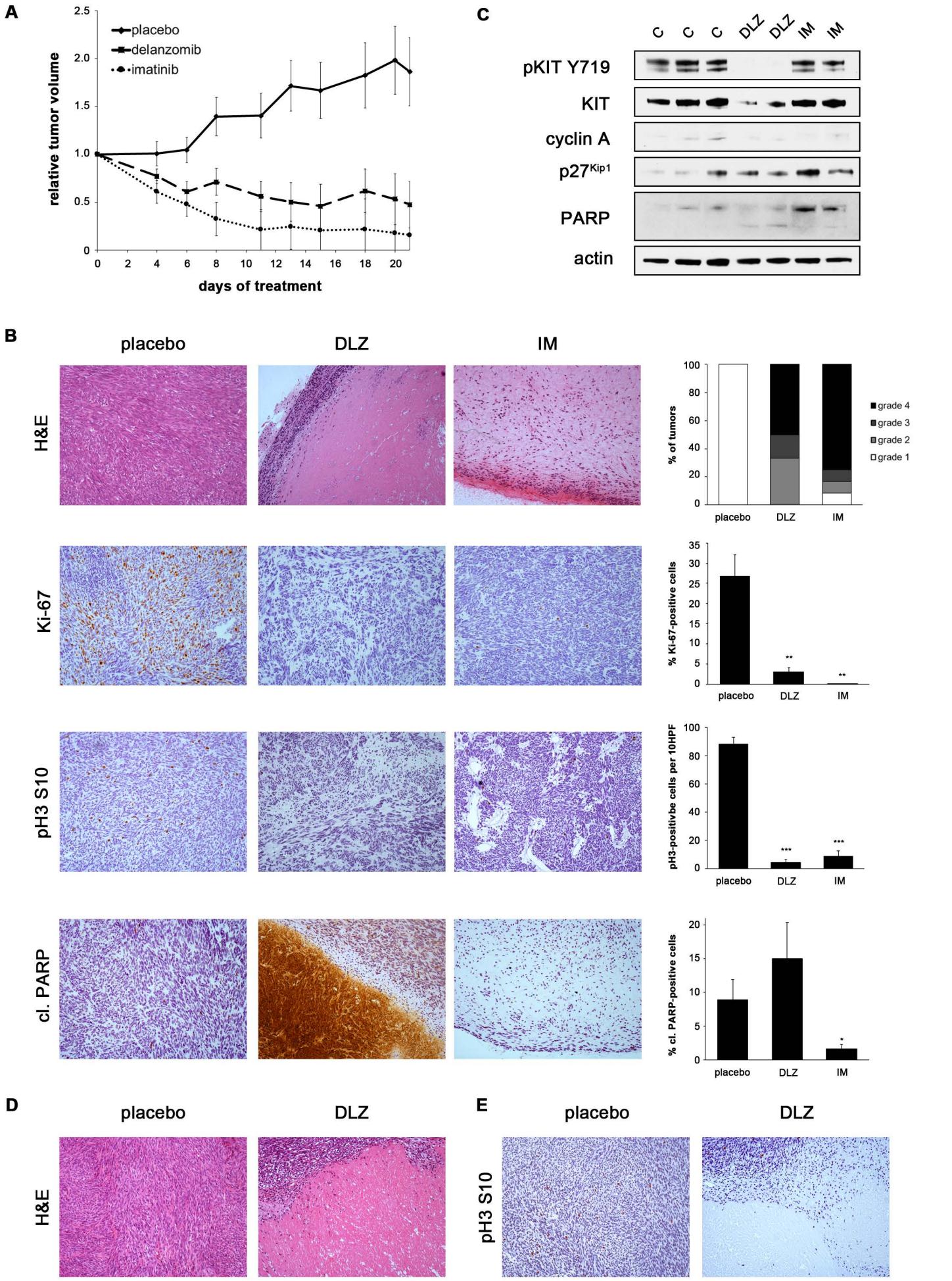

Rausch *et al.*, Figure 5